

**A VUV Photoionization Study of the Combustion-Relevant Reaction of the
Phenyl Radical (C₆H₅) with Propylene (C₃H₆) in a High Temperature
Chemical Reactor**

Fangtong Zhang, Ralf I. Kaiser*

Department of Chemistry, University of Hawaii at Manoa, Honolulu, HI

Amir Golan, Musahid Ahmed*

Chemical Sciences Division, Lawrence Berkeley National Laboratory, Berkeley, CA

Nils Hansen

Combustion Research Facility, Sandia National Laboratories, Livermore, CA

JPCA (submitted February 2012)

ABSTRACT

We studied the reaction of phenyl radicals (C_6H_5) with propylene (C_3H_6) exploiting a high temperature chemical reactor under combustion-like conditions (300 Torr, 1,200-1,500 K). The reaction products were probed in a supersonic beam by utilizing tunable vacuum ultraviolet (VUV) radiation from the Advanced Light Source and recording the photoionization efficiency (PIE) curves at mass-to-charge ratios of $m/z = 118$ ($C_9H_{10}^+$) and $m/z = 104$ ($C_8H_8^+$). Our results suggest that the methyl and atomic hydrogen losses are the two major reaction pathways with branching ratios of $86 \pm 10 \%$ and $14 \pm 10 \%$. The isomer distributions were probed by fitting the recorded PIE curves with a linear combination of the PIE curves of the individual C_9H_{10} and C_8H_8 isomers. Styrene ($C_6H_5C_2H_3$) was found to be the *exclusive* product contributing to $m/z = 104$ ($C_8H_8^+$), whereas 3-phenylpropene, *cis*-1-phenylpropene, and 2-phenylpropene with branching ratios of $96 \pm 4 \%$, $3 \pm 3 \%$, and $1 \pm 1 \%$ could account for signal at $m/z = 118$ ($C_9H_{10}^+$). Although searched for carefully, no evidence of the bicyclic indane molecule could be provided. The reaction mechanisms and branching ratios are explained in terms of electronic structure calculations nicely agreeing with a recent crossed molecular beam study on this system.

1. Introduction

As precursors of soot as well as their importance in combustion,¹⁻³ atmospheric^{4,5} and interstellar chemistry,⁶⁻⁸ the formation routes to polycyclic aromatic hydrocarbons (PAHs) have received considerable attention.^{9,10} It is widely accepted that the phenyl radical, $C_6H_5(X^2A_1)$, represents a crucial building block to yield the second ring thus initiating the formation of PAHs and related molecules such as (partially) hydrogenated and/or dehydrogenated PAHs in combustion systems.¹¹⁻¹³ In detail, PAHs have been suggested to be formed via hydrogen abstraction - acetylene addition (HACA) sequences¹⁴ or via phenyl addition - cyclization pathways (PAC).¹⁵ Alternative pathways have been investigated via kinetic studies¹⁶⁻¹⁹ and crossed beam experiments²⁰⁻²³ of phenyl radicals with unsaturated hydrocarbons. Very recently, indane has been identified as one of the products in a low-pressure premixed toluene/oxygen/ argon fuel rich flames by Li et al. at 2009.²⁴ The aromatic, bicyclic indane molecule as well as its α -methylstyrene (2-phenylpropene) and 1-phenylpropene isomers are considered as important reaction intermediates and toxic byproducts in the combustion of fossil fuel (Figure 1).^{11,12,25-32} The reaction of the phenyl radical (C_6H_5) with propylene (C_3H_6) presents a potential synthetic routes to synthesize C_9H_{10} isomers and to access the C_9H_{11} potential energy surface.

As early as in 1972, Hefter et al.³³ investigated this system in liquid propylene at 183 K utilizing electron spin resonance. In 2006, Park et al.¹⁷ conducted a kinetics study exploiting cavity ring-down spectroscopy at temperatures between 296 and 496 K combined with ab initio calculations; in 2008, Kaiser et al. conducted a crossed beam experiment of this system at elevated collision energies of 130 to 190 kJ mol^{-1} .²¹ All three studies agreed that this reaction was initiated by an addition of the phenyl radical predominantly to the C1-carbon atom of the propylene molecule at the $=CH_2$ unit to form a doublet radical intermediate; the latter ejected a hydrogen atom via a rather loose exit transition state forming solely monocyclic C_9H_{10} isomers. No methyl group loss was observed at elevated collision energies. Most recently, our group re-investigated this reaction utilizing a crossed beam method at a much lower collision energy of about 45 kJ mol^{-1} .³⁴ The methyl group loss channel yielding styrene was successfully identified, and a fraction of the methyl versus hydrogen loss channels of $68 \pm 6\%$ to $32 \pm 10\%$ was derived experimentally agreeing nicely with RRKM theory. Apart from crossed beam,^{20-22,35} flame^{10,36,37} and shock tube³⁸⁻⁴⁰ studies, reactions carried out under pyrolytic conditions present an excellent

complementary approach to simulate combustion-like conditions and to investigate the formation mechanisms of PAHs.^{41,42} In 2008, Shukla et al.¹⁵ conducted an investigation on the basis of a kinetic analysis of gas phase products of pyrolysis of benzene with and without addition of acetylene. Reactions were conducted in a flow tube, and the products were probed in situ by a *direct sampling* mass spectrometric technique using vacuum ultraviolet (VUV) single photon ionization (SPI) time of flight mass spectrometry (TOF-MS). The authors found that the PAC pathway presented a highly efficient growth mechanism to form PAHs. The products included PAHs up to 454 amu ($C_{36}H_{22}$). Especially, acetylene was mixed with benzene to understand the impact of HACA on the PAC pathways; this resulted in an enhancement of PAH production in spite of trapping of active and chain-carrier species such as the phenyl radical by acetylene to form phenylacetylene. The comparison of both the HACA and PAC mechanisms concluded that PAC is a highly efficient mechanism for the growth of PAHs.

Recently, we studied the reaction of phenyl (C_6H_5) with methylacetylene (CH_3CCH) and allene (H_2CCCH_2) exploiting a high temperature chemical reactor under combustion-like conditions (300 Torr, 1,200-1,500 K).⁴³ The product isomer distributions were probed utilizing tunable VUV radiation from the Advanced Light Source (ALS) by recording the photoionization efficiency (PIE) curves at mass-to-charge of $m/z = 116$ ($C_9H_8^+$) of the products in a supersonic expansion. Branching ratios were derived by fitting the recorded PIE curves with a linear combination of the individual C_9H_8 isomer PIE curves. In both reactions, the aromatic indene molecule was identified. In this paper we expand on these studies systematically by decreasing the carbon-to-hydrogen ratio of the closed shell reactant from 0.75 (methylacetylene, allene) to 0.5 (propylene) and report on the results of the phenyl-propene reaction utilizing the very same pyrolytic reactor. Recall that in case of distinct structural isomers, the adiabatic ionization energy (IE) and the corresponding PIE curves, which report the ion signal of $m/z = 116$ ($C_9H_{10}^+$) of a distinct isomer versus the photon energy, can differ dramatically. By photoionizing the neutral C_9H_{10} products in the supersonic molecular beam via tunable vacuum ultraviolet (VUV) radiation from the Advanced Light Source at various photon energies, we measured PIEs of $m/z = 118$ ($C_9H_{10}^+$) and $m/z = 104$ ($C_8H_8^+$). These PIE curves are the result of a linear combination of the individual isomer PIE curves present in the supersonic beam and hence we can identify the products formed in the reactions of phenyl radicals with propylene and extract their branching ratios.

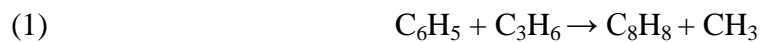
2. Experimental

The central device of the experiments is a resistively heated high temperature ‘chemical reactor’⁴⁴ incorporated into the molecular beams end station at the Chemical Dynamics Beamline (9.0.2.) of the Advanced Light Source. Briefly, this setup allows a simulation of combustion-relevant conditions such as temperature and pressure as well as chemical reactions to form combustion-relevant molecules such as PAHs and their isomers *in situ*. Here, a continuous beam of phenyl radicals (C_6H_5) was generated *in situ* via quantitative pyrolysis of nitrosobenzene (C_6H_5NO ; Aldrich) - held at 293 K - seeded in neat propylene carrier gas (C_3H_6 ; Sigma), which was expanded at a pressure of 300 Torr through a 0.1 mm orifice into a resistively heated silicon carbide (SiC) tube with an inner diameter of 1 mm and a length of 20 mm. A heating current of 1.3 A was applied to the silicon carbide tube reflecting an operating power of 20 W. An independent temperature calibration of the pyrolytic source with pure helium carrier gas coupled to a time-of-flight mass spectrometer and chopper wheel suggested temperatures of 1,200 – 1,500 K of the silicon carbide tube. In the present experiments, we would like to stress that propylene did not only act as a seeding gas, but also as a reactant with the pyrolytically generated phenyl radicals. Considering the length of the tube of 2.0 ± 0.1 cm and a thermal, non-supersonic velocity of the propylene reactant at $1,350 \pm 150$ K inside the tube of 900 ± 50 ms^{-1} , we estimate a residence time of the reactants in the silicon carbide tube of 24 ± 2 μs . The setup allows an analysis of the *in situ* generated products. Here, after passing a 2 mm skimmer located 10 mm downstream from the silicon carbide nozzle, quasi continuous tunable VUV radiation from the ALS crossed the neutral molecular beam at the extraction region of a Wiley–McLaren Reflectron Time-of-Flight (Re-TOF) mass spectrometer 55 mm downstream. The ions of the photoionized molecules were then extracted and collected by a microchannel plate detector in the Re-TOF mode utilizing a multi channel scaler. The PIE curves were obtained by plotting the integrated relevant ion counts at a desired mass-to-charge, m/z , versus the photoionization energy between 8.0 and 10.1 eV in steps of 0.1 eV. The signal was normalized to the photon flux. Based on calibrated PIE curves of expected products of a well-defined molecular mass and their acyclic isomers ($m/z = 118$; C_9H_{10}), the recorded PIE curves were then fit via a linear combination with known PIE curves of various C_9H_{10} isomers to extract the nature of the products formed and their branching ratios.

In order to fit the PIE curve at $m/z = 118$ (C_9H_{10}) obtained during the phenyl – propylene experiment, we also recorded the PIE curves of the individual C_9H_{10} isomers, which are not available from the literature (Electronic Supplementary Material) (Figure 1). Briefly, the PIE curves of five C_9H_{10} isomers indane (TCI, 98%), 3-phenylpropene (TCI, 98%), *cis/trans*-1-phenylpropene (TCI, 98%), and α -methylstyrene (2-phenylpropene) (Sigma Aldrich, 98%) were recorded also at the Chemical Dynamics Beamline (9.0.2.) of the Advanced Light Source. For each isomer, a continuous beam of the C_9H_{10} isomer was generated by passing helium (Airgas, 99.999 %) carrier gas with a pressure of 300 Torr through a home-made stainless steel bubbler, which contained the individual C_9H_{10} isomer at 293 K. This gas mixture expanded through a 0.1 mm orifice into the source chamber before passing a 2 mm skimmer 10 mm downstream to reach the detector chamber. As for the reaction products, the ions of the photoionized molecules were then extracted and collected by a microchannel plate detector in the Re-TOF mode. Individual PIE curves were obtained by plotting the integrated ion counts $m/z = 118$ versus the photoionization energy between 8.00 eV and 10.10 eV in steps of 0.025/0.01 eV. The signal was normalized to the photon flux. The PIE curves of the five C_9H_{10} isomers are presented in the Electronic Supplementary Material. The ionization energies were derived to be 8.42, 8.40, 8.28, 8.38, and 8.23 eV for indane, 3-phenylpropene, *cis/trans*-1-phenylpropene, and α -methylstyrene, respectively. These values can be compared with NIST data of 8.45, 8.2~8.7, 8.5, 8.3 and 8.3, respectively.⁴⁵

3. Results and Discussion

The mass spectra of the species formed in the supersonic expansion and the PIE curves of $m/z = 118$ ($C_9H_{10}^+$) and $m/z = 104$ ($C_8H_8^+$) are shown in Figures 2 and in Figure 3, respectively. Apart from signal at $m/z = 30$ (NO) and $m/z = 42$ (C_3H_6), the mass spectrum depicts peaks at $m/z = 104$ and 118 corresponding to $C_8H_8^+$ and $C_9H_{10}^+$, respectively. These products are formed via the methyl and hydrogen loss channels, respectively, in the reaction of phenyl radicals with propylene (equations (1) and (2)). The branching ratios of both channels are estimated from the peak intensities and scaled photon absorption cross sections⁴⁶ to be about $86 \pm 10 \% : 14 \pm 10 \%$.



Note that the peak at $m/z = 94$ might correspond to phenol, which is likely produced in the reactions involving the nitrogen monoxide by-product formed in the pyrolysis of nitrosobenzene.

As discussed above, the major products of the phenyl - propene reaction hold the molecular formulae C_8H_8 and C_9H_{10} . We attempt now to fit the recorded PIEs with a linear combination of PIEs of the corresponding isomers. The PIE curve of $m/z = 104$ (C_8H_8) can be reproduced exclusively with the literature PIE curve of styrene ($C_6H_5C_2H_3$). The experimentally recorded PIE curve of $m/z = 118$ (C_9H_{10}) can be principally fit with the PIE of the 3-phenylpropene isomer. Fractions of cis-1-phenylpropene and 2-phenylpropene at the few per cent level slightly improve the fit with an overall branching ratio of 3-phenylpropene, cis-1-phenylpropene, and 2-phenylpropene of $96 \pm 4 \%$, $3 \pm 3 \%$, and $1 \pm 1 \%$. Noticeably, there is no evidence of the formation of the bicyclic indane molecule. This is in contrary to the phenyl-allene/propyne reactions, in which the bicyclic indene molecule was identified.⁴³

In an attempt to understand the predominant formation of 3-phenylpropene and styrene, we inspected the underlying potential energy surface (PES).³⁴ As predicted computationally, the phenyl - propene reaction is likely initiated either by the phenyl addition of the phenyl radical with its unpaired electron to the sterically less hindered CH_2 group of the propylene molecule to form the **i1** intermediate located 152 kJ mol^{-1} below the reactants via a 6.3 kJ mol^{-1} barrier; alternatively, phenyl can add to the CH group of propylene yielding the **i2** intermediate, which is almost isoenergetic to **i1** and placed 147 kJ mol^{-1} below the reactants via a higher 11.3 kJ mol^{-1} barrier. Both **i1** and **i2** intermediates are interconvertible via intermediate **i3**. Intermediate **i1** can eject a hydrogen atom from the methyl group to form the 3-phenylpropene product. This reaction channel is overall exoergic by 13 kJ mol^{-1} . From the **i2** intermediate, a methyl group can be ejected to yield the styrene product. Besides those two major reaction pathways highlighted via bold arrows in Figure 4, two minor pathways were identified. First, **i1** can lose a hydrogen atom from the adjacent CH_2 group to form cis-1-phenylpropene molecule; this channel is exoergic by 24 kJ mol^{-1} . Further, **i2** can emit atomic hydrogen and form 2-phenylpropene. It can be seen that in order to access the bicyclic indane molecule, the reaction has to go through a multi-step pathway involving $i1 \rightarrow i4 \rightarrow i7 \rightarrow \text{indane} + H$; more importantly, the barrier between **i1** and **i4** is located 21 kJ mol^{-1} above the reactants; due to this barrier, the pathway to form indane is less likely than yielding 3-phenylpropene and styrene. Also, intermediate **i1** is critical to form indane.

However, considering the barriers for the competing pathways **i1** might follow, **i1** rather fragments to 3-phenylpropene plus atomic hydrogen instead of pursuing the reaction sequence **i1** → **i4** → **i7** → indane plus hydrogen. This reaction scheme correlates well with our experimental results, in which styrene and 3-phenylpropene are identified as the two major products, as well as the cis-1-phenylpropene and 2-phenylpropene molecules possibly existing at small fractions at the per cent level. Also, no indane molecule was observed. Compared to the recent crossed beam reaction, of phenyl with propylene,³⁴ the results also agree very nicely. First, the branching ratios of the methyl and hydrogen loss pathways were determined to be $68 \pm 16\%$ and $32 \pm 10\%$, respectively, under single collision conditions at a collision energy of about 45 kJ mol^{-1} . Further, the crossed beam reaction did not depict any evidence of indane formation.

We would like to highlight that little is known about the combustion chemistry of the phenylpropene system. As a matter of fact, although the reaction product styrene has been detected in combustion flames, the 3-phenylpropene molecule, formed via the phenyl radical – atomic hydrogen replacement pathway, has not been included in any of the commonly used combustion chemistry models. Nevertheless, these species could contribute to molecular-weight growth in combustion processes: hydrogen-abstraction reactions from the experimentally observed phenylpropene isomers provide conceivable pathways to phenyl-substituted allyl radicals: 1-phenylallyl and 2-phenylallyl. Similar to benzene and fulvene formation via the propargyl - allyl or allyl - allyl reactions, phenyl-substituted allyl radicals could provide pathways to biphenyl or triphenyl involving reactions with propargyl (or allyl) or phenyl-substituted allyl radicals. Likewise, hydrogen atoms as present in combustion flames, might change the spectrum of the primary reaction products and could lead via hydrogen addition – isomerization – hydrogen elimination to the indane molecule. Alternatively, the indane molecule as observed in combustion flames might be formed via hydrogenation of indene, with the latter being formed in the phenyl – allene and phenyl – methylacetylene reactions.

4. Conclusions

We investigated the combustion-relevant reaction of phenyl radicals (C_6H_5) with propylene (C_3H_6) exploiting a high temperature chemical reactor under combustion-like conditions at

temperatures of about 1,200 to 1,500 K. The reaction products were probed in a supersonic beam by utilizing tunable VUV radiation from the Advanced Light Source and recording the PIE curves at mass-to-charge ratios of $m/z = 118$ ($C_9H_{10}^+$) and $m/z = 104$ ($C_8H_8^+$). Our results indicate that the methyl and atomic hydrogen losses are the two major reaction pathways with branching ratios of $86 \pm 10 \%$ and $14 \pm 10 \%$. Styrene ($C_6H_5C_2H_3$) was found to be the *exclusive* product contributing to $m/z = 104$ ($C_8H_8^+$), whereas 3-phenylpropene, cis-1-phenylpropene, and 2-phenylpropene with branching ratios of $96 \pm 4 \%$, $3 \pm 3 \%$, and $1 \pm 1 \%$ could account for signal at $m/z = 118$ ($C_9H_{10}^+$). No evidence of the bicyclic indane molecule could be provided. These isomers could contribute to molecular-weight growth in combustion processes since hydrogen-abstraction reactions from the phenyl-propene isomers provide viable pathways to phenyl-substituted allyl radicals. These are: 1-phenyl-allyl and 2-phenyl-allyl. These phenyl-substituted allyl radicals could provide pathways to biphenyl or triphenyl involving reactions with propargyl (or allyl) or phenyl-substituted allyl radicals.

ACKNOWLEDGEMENTS

This research was supported by the US Department of Energy Office of Science via projects DE-FG02-03-ER15411 (RIK, FZ). MA and AG are supported by the Office of Science, Office of Basic Energy Sciences, of the US Department of Energy under Contract No. DE-AC02-05CH11231, through the Chemical Sciences Division. The Advanced Light Source is supported by the Director, Office of Science, Office of Basic Energy Sciences, of the U.S. Department of Energy under Contract No. DE-AC02-05CH11231. Sandia is a multi-program laboratory operated by Sandia Corporation, a Lockheed Martin Company, for the National Nuclear Security Administration under contract DE-AC04-94-AL85000.

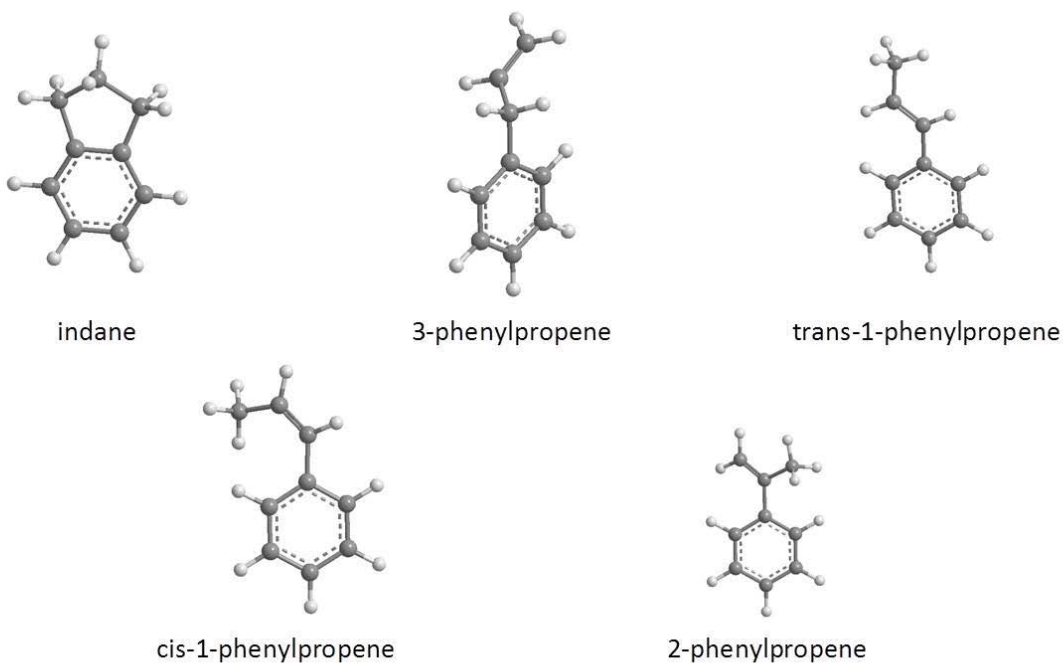


Figure 1: Structures of distinct C₉H₁₀ isomers potentially formed in the reaction of phenyl radicals with propylene.

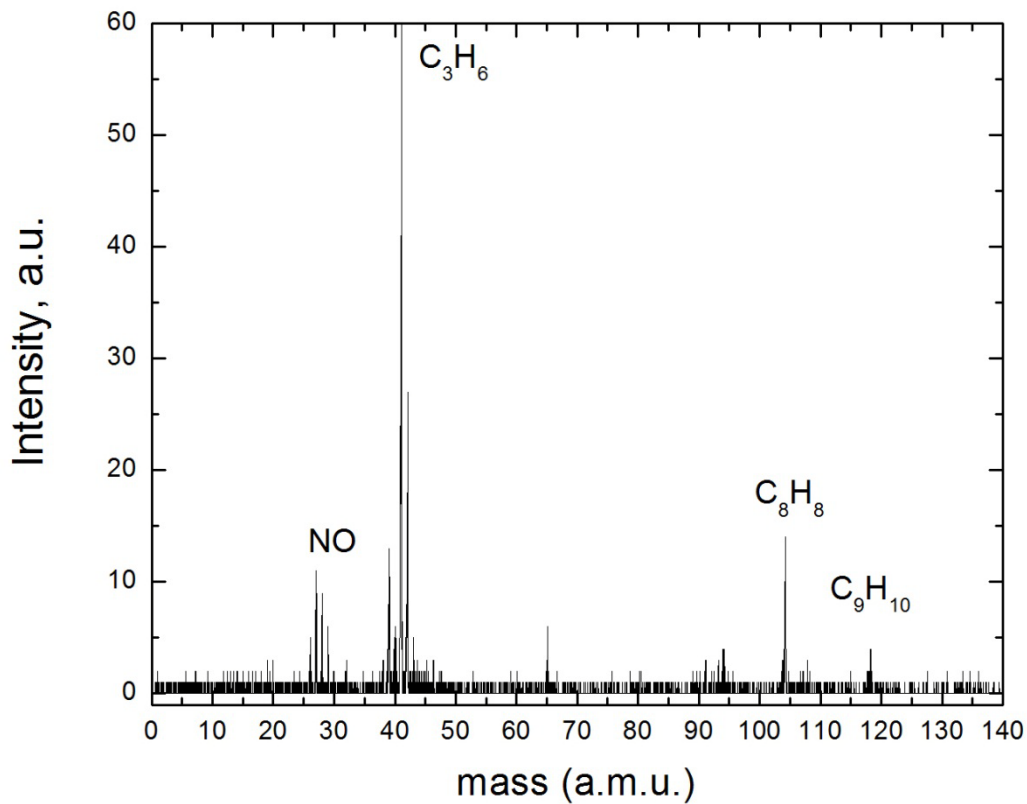


Figure 2: Mass spectrum of the products of the phenyl-propene pyrolytic reaction recorded at a photon energy of 8.6 eV. Note that the mass spectrum of the non-pyrolyzed gas mixture recorded at a photon energy of XXX eV depicted ion counts for both propylene ($m/z = 42$) and nitrosobenzene ($m/z = 107$).

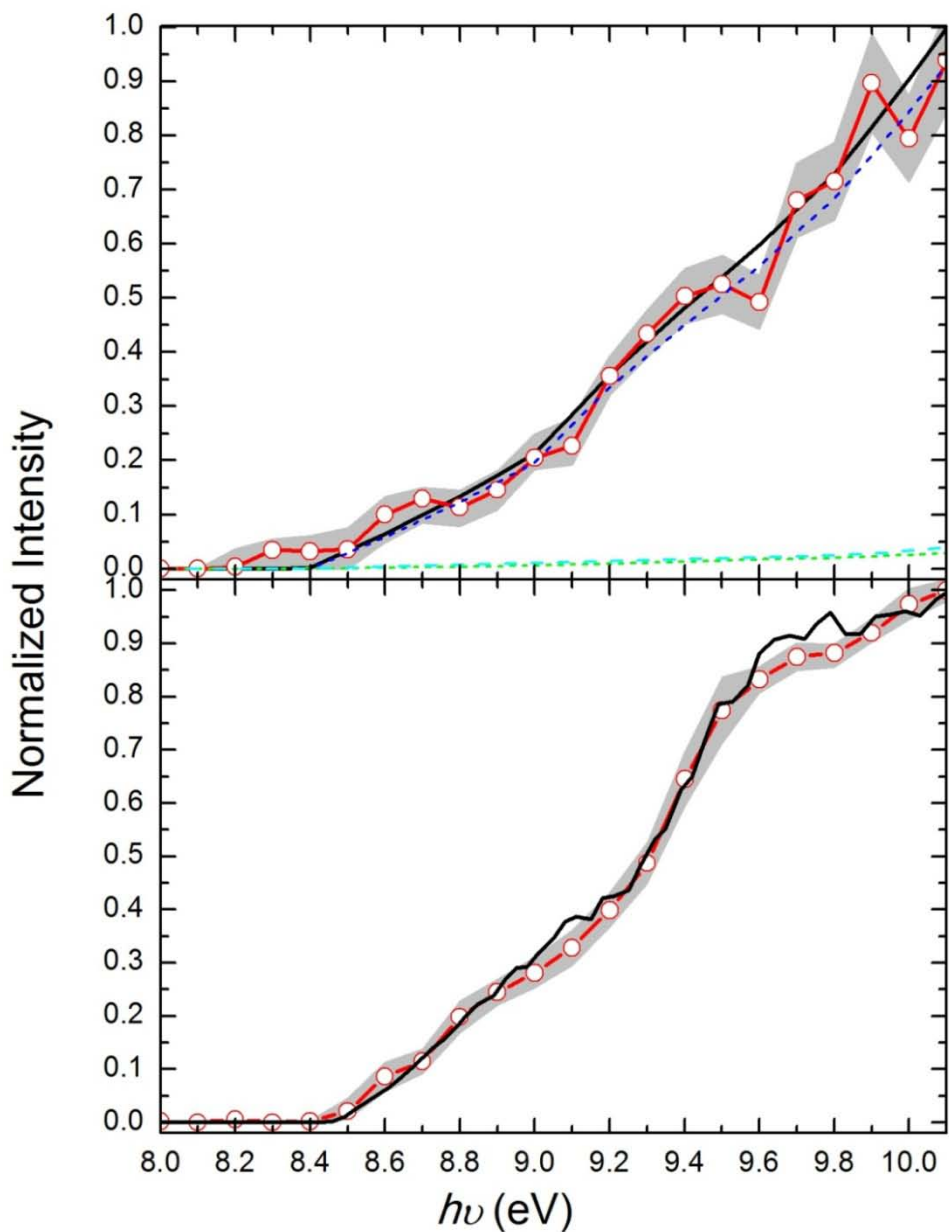


Figure 3. Upper panel: the red circles and line presents the PIE obtained at $m/z = 118$, whereas the black line is the simulation using PIEs of 3-phenylpropene (blue), cis-1-phenylpropene (green) and 2-phenylpropene (cyan). Lower panel: the red circles and line presents the PIE obtained at $m/z = 104$; the PIE curve of styrene is taken from reference.⁴⁶ Experimental errors are defined by the grey curve.

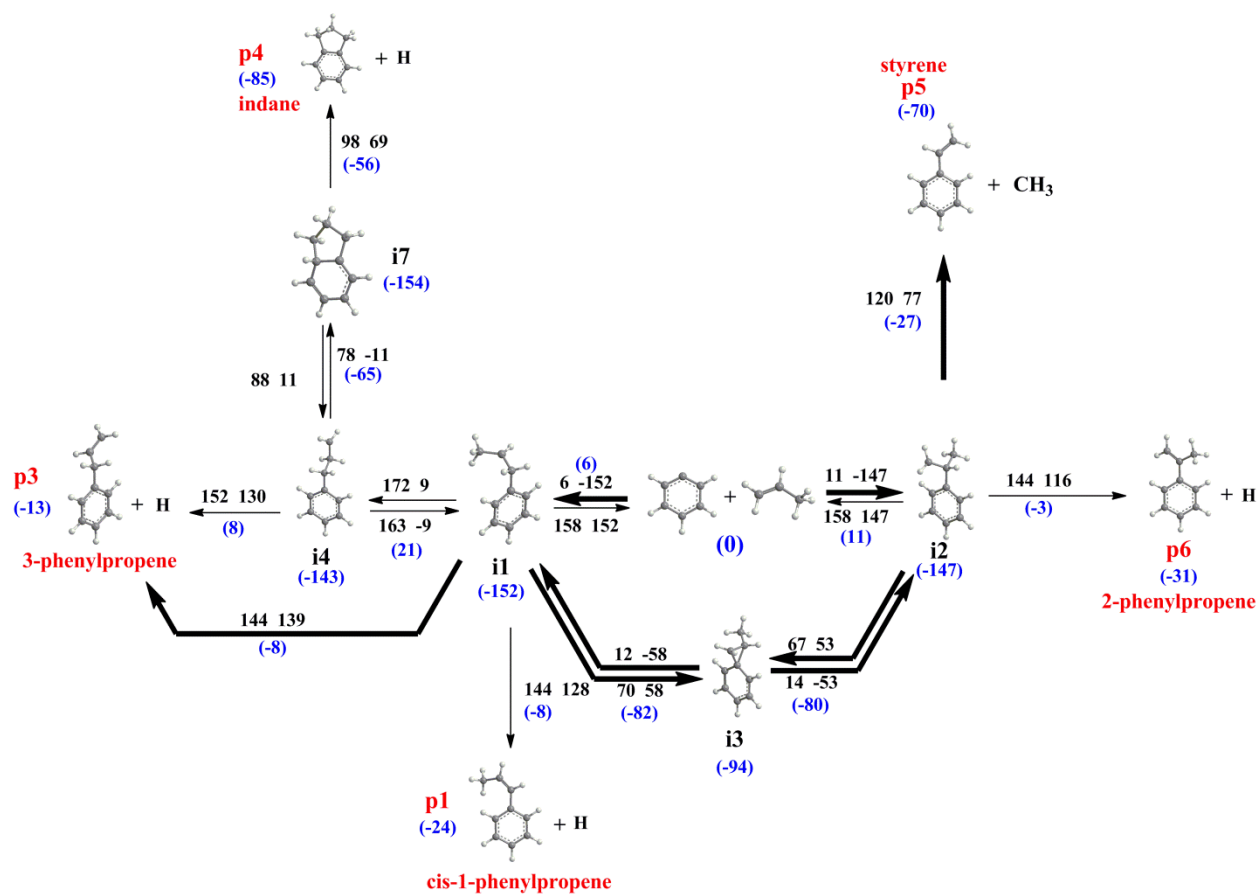


Figure 4. Relevant parts of the potential energy surface of the phenyl plus propene reaction taken from Reference 34. All relative energies (shown in blue color online and in parentheses, in kJ mol^{-1}) are calculated at the G3(MP2,CC)//B3LYP/6-311G(d,p) + ZPE(B3LYP/6-311G(d,p)) level of theory. The numbers next to the arrows show the barrier (first) and the reaction energy (second) for each individual step in kJ mol^{-1} .

References:

- (1) Goldaniga, A.; Faravelli, T.; Ranzi, E. *Combust.* **2000**, *122*, 350-358.
- (2) Marinov, N. M.; Pitz, W. J.; Westbrook, C. K.; Castaldi, M. J.; Senkan, S. M. *Combust. Sci. Technol.* **1996**, *116-117*, 211-287.
- (3) Sye, W. F.; Lin, C. L.; Yen, D. P.; Tsai, C. S. *J. Chin. Chem. Soc. (Taipei)* **1988**, *35*, 1-11.
- (4) Ergut, A.; Levendis, Y. A.; Richter, H.; Carlson, J. "Investigation of soot onset threshold in one-dimensional, laminar, atmospheric pressure, premixed, ethylbenzene flames", 2005.
- (5) Atkinson, R.; Arey, J. *Environ. Health Perspect. Suppl.* **1994**, *102*, 117-126.
- (6) Kaiser, R. I. *Abstracts of Papers, 231st ACS National Meeting, Atlanta, GA, United States, March 26-30, 2006* **2006**, PHYS-080.
- (7) Wakelam, V.; Herbst, E. *Astrophys. J.* **2008**, *680*, 371-383.
- (8) Helling, C.; Joergensen, U. G.; Plez, B.; Johnson, H. R. *Astron. Astrophys.* **1996**, *315*, 194-203.
- (9) Frenklach, M.; Feigelson, E. D. *Astrophys. J.* **1989**, *341*, 372-384.
- (10) Richter, H.; Howard, J. B. *Progress in Energy and Combustion Science* **2000**, *26*, 565-608.
- (11) Lindstedt, P.; Maurice, L.; Meyer, M. *Faraday Discuss* **2001**, 409-432; discussion 445-459.
- (12) Kamphus, M.; Braun-Unkloff, M.; Kohse-Hoeinghaus, K. *Combust. Flame* **2008**, *152*, 28-59.
- (13) Frenklach, M. *Physical Chemistry Chemical Physics* **2002**, *4*, 2028-2037.
- (14) Bockhorn, H.; Fetting, F.; Heddrich, A.; Wannemacher, G. *Ber. Bunsen-Ges. Phys. Chem.* **1987**, *91*, 819-825.
- (15) Shukla, B.; Susa, A.; Miyoshi, A.; Koshi, M. *J. Phys. Chem. A* **2008**, *112*, 2362-2369.
- (16) Yu, T.; Lin, M. C. *Combust. Flame* **1995**, *100*, 169-176.
- (17) Park, J.; Nam, G. J.; Tokmakov, I. V.; Lin, M. C. *J. Phys. Chem. A* **2006**, *110*, 8729-8735.
- (18) Tokmakov, I. V.; Park, J.; Lin, M. C. *ChemPhysChem* **2005**, *6*, 2075-2085.
- (19) Park, J.; Wang, L.; Lin, M. C. *Int. J. Chem. Kinet.* **2003**, *36*, 49-56.
- (20) Gu, X.; Kaiser, R. I. *Acc. Chem. Res.* **2009**, *42*, 290-302.
- (21) Zhang, F.; Gu, X.; Guo, Y.; Kaiser, R. I. *J. Phys. Chem. A* **2008**, *112*, 3284-3290.
- (22) Zhang, F.; Gu, X.; Guo, Y.; Kaiser, R. I. *J. Org. Chem.* **2007**, *72*, 7597-7604.
- (23) Gu, X.; Zhang, F.; Guo, Y.; Kaiser, R. I. *Angew. Chem., Int. Ed.* **2007**, *46*, 6866-6869.
- (24) Li, Y.; Zhang, L.; Tian, Z.; Yuan, T.; Wang, J.; Yang, B.; Qi, F. *Energy Fuels* **2009**, *23*, 1473.
- (25) Newby, J. J.; Stearns, J. A.; Liu, C.-P.; Zwier, T. S. *J. Phys. Chem. A* **2007**, *111*, 10914-10927.
- (26) Li, Y.; Tian, Z.; Zhang, L.; Yuan, T.; Zhang, K.; Yang, B.; Qi, F. *Proc. Combust. Inst.* **2009**, *32*, 647-655.
- (27) Li, Y.; Zhang, L.; Tian, Z.; Yuan, T.; Wang, J.; Yang, B.; Qi, F. *Energy Fuels* **2009**, *23*, 1473-1485.

- (28) Li, Y.; Zhang, L.; Tian, Z.; Yuan, T.; Zhang, K.; Yang, B.; Qi, F. *Proc. Combust. Inst.* **2009**, *32*, 1293-1300.
- (29) Li, Y.; Zhang, L.; Yuan, T.; Zhang, K.; Yang, J.; Yang, B.; Qi, F.; Law, C. K. *Combust. Flame* **2010**, *157*, 143-154.
- (30) Verevkin, S. P.; Emel'yanenko, V. N.; Pimerzin, A. A.; Vishnevskaya, E. E. *J. Phys. Chem. A* **2011**, *115*, 1992-2004.
- (31) Pousse, E.; Tian, Z. Y.; Glaude, P. A.; Fournet, R.; Battin-Leclerc, F. *Combust. Flame* **2010**, *157*, 1236-1260.
- (32) Richter, H.; Howard, J. B. *Prog. Energy Combust. Sci.* **2000**, *26*, 565-608.
- (33) Hefter, H. J.; Hecht, T. A.; Hammond, G. S. *J. Am. Chem. Soc.* **1972**, *94*, 2793.
- (34) Kaiser, R. I.; Parker, D. S. N.; Goswami, M.; Zhang, F.; Kislov, V. V.; Mebel, A. M.; Aguilera-Iparraguirre, J.; Green, W. H. *Phys. Chem. Chem. Phys.* **2012**, *14*, 720-729.
- (35) Gu, X.; Guo, Y.; Mebel, A. M.; Kaiser, R. I. *Chem. Phys. Lett.* **2007**, *449*, 44-52.
- (36) Carstensen, H. H.; Dean, A. M.; Yeh, L. I.; Takatori, Y.; Akihama, K. *Prepr. - Am. Chem. Soc., Div. Pet. Chem.* **1998**, *43*, 602-606.
- (37) Hansen, N.; Klippenstein, S. J.; Westmoreland, P. R.; Kasper, T.; Kohse-Hoinghaus, K.; Wang, J.; Cool, T. A. *Phys. Chem. Chem. Phys.* **2008**, *10*, 366-374.
- (38) Wang, H. *Int. J. Chem. Kinet.* **2001**, *33*, 698-706.
- (39) Bentz, T.; Giri, B. R.; Hippler, H.; Olzmann, M.; Striebel, F.; Szoeri, M. *J. Phys. Chem. A* **2007**, *111*, 3812-3818.
- (40) Kern, R. D.; Xie, K.; Chen, H. *Combust. Sci. Technol.* **1992**, *85*, 77-86.
- (41) Yuan, T.; Zhang, L.; Zhou, Z.; Xie, M.; Ye, L.; Qi, F. *The Journal of Physical Chemistry A* **2011**, *115*, 1593.
- (42) Ammann, J. R.; Britt, P. F.; Buchanan, A. C., III. *Prepr. Symp. - Am. Chem. Soc., Div. Fuel Chem.* **1999**, *44*, 248-250.
- (43) Zhang, F.; Kaiser, R. I.; Kislov, V. V.; Mebel, A. M.; Golan, A.; Ahmed, M. *Journal of Physical Chemistry Letters* **2011**, *2*, 1731-1735.
- (44) Kohn, D. W.; Clauberg, H.; Chen, P. *Rev. Sci. Instrum.* **1992**, *63*, 4003-4005.
- (45) Linstrom, P. J.; Mallard, W. G. NIST Chemistry WebBook. In *NIST Standard Reference Database Number 69*; National Institute of Standards and Technology: Gaithersburg, MD, June 2005.
- (46) Zhou, Z.; Xie, M.; Wang, Z.; Qi, F. *Rapid Commun. Mass Spectrom.* **2009**, *23*, 3994.

This document was prepared as an account of work sponsored by the United States Government. While this document is believed to contain correct information, neither the United States Government nor any agency thereof, nor the Regents of the University of California, nor any of their employees, makes any warranty, express or implied, or assumes any legal responsibility for the accuracy, completeness, or usefulness of any information, apparatus, product, or process disclosed, or represents that its use would not infringe privately owned rights. Reference herein to any specific commercial product, process, or service by its trade name, trademark, manufacturer, or otherwise, does not necessarily constitute or imply its endorsement, recommendation, or favoring by the United States Government or any agency thereof, or the Regents of the University of California. The views and opinions of authors expressed herein do not necessarily state or reflect those of the United States Government or any agency thereof or the Regents of the University of California.